Wirelessly Powered Backscatter Communication Networks: Modeling, Coverage and Capacity

Kaifeng Han and Kaibin Huang
Department of Electrical and Electronic Engineering
The University of Hong Kong, Hong Kong
Email: kfhan@eee.hku.hk, huangkb@eee.hku.hk

***Abstract*—Future Internet-of-Things (IoT) will connect billions of small computing devices embedded in the environment and support their device-to-device (D2D) communication. Powering this massive number of embedded devices is a key challenge of designing IoT since batteries increase the devices' form factors and their recharging/replacement is difficult. To tackle this challenge, we propose a novel network architecture that integrates wireless power transfer and backscatter communication, called *wirelessly powered backscatter communication* (WP-BC) networks. In this architecture, *power beacons* (PBs) are deployed for wirelessly powering devices; their *ad-hoc* communication relies on backscattering and modulating incident continuous waves from PBs, which consumes orders-of-magnitude less power than traditional radios. Thereby, the dense deployment of low-complexity PBs with high transmission power can power a large-scale IoT. In this paper, a WP-BC network is modeled as a random Poisson cluster process in the horizontal plane where PBs are Poisson distributed and active ad-hoc pairs of backscatter communication nodes with fixed separation distances form random clusters centered at PBs. Furthermore, by harvesting energy from and backscattering radio frequency (RF) waves transmitted by PBs, the transmission power of each node depends on the distance from the associated PB. Applying stochastic geometry, the network coverage probability and transmission capacity are derived and optimized as functions of the backscatter reflection coefficient and duty cycle as well as the PB density. The effects of the parameters on network performance are characterized.**

I. Introduction

The vision of *Internet-of-Things* (IoT) is to connect billions of small computing devices embedded in the environment (e.g., walls and furniture) and implanted in bodies and enable their *device-to-device* (D2D) wireless communication. Powering a massive number of such devices is a key design challenge for IoT. Batteries add to their weights and form factors and battery recharging/replacement increases the maintenance cost if not infeasible. To tackle the challenge, we propose a novel network architecture that enables large-scale passive IoT deployment by seamless integration of wireless power transfer (WPT) [1], [2] and low-power backscattering communication, called a *wirelessly powered backscatter communication* (WP-BC) network. Specifically, *power beacons* (PBs) that are stations dedicated for WPT [3] are deployed for wirelessly powering dense backscatter D2D links and each node transmits data by reflecting and modulating the carrier signal sent by PBs. In this paper, a large-scale WP-BC network is modeled as Poisson cluster processes and its coverage and capacity are analyzed using stochastic geometry.

Backscatter communication refers to a design where a radio device transmits data via reflecting and modulating an incident radio frequency (RF) signal by adapting the level of antenna impedance mismatch to vary the reflection coefficient and furthermore harvests energy from the signal [4], [5]. As their require no energy hungry components such as oscillators and analog-to-digital converters (ADCs), a backscatter transmitter consumes power orders-of-magnitude less than a conventional radio. Traditionally, backscatter communication is widely used in the application of radio frequency Identification (RFID) where a reader powers and communicates with a RFID tag over a short range typically of several meters [5]–[7]. This design is unsuitable for IoT since typical nodes are energy constrained and may not be able to wirelessly power other nodes for communications over sufficiently long distances. This motivated the design of backscatter communication powered by RF energy harvesting where the transmission of a backscatter node relies on reflecting incident RF signals from the ambient environment such as TV, Wi-Fi and cellular signals [8], [9]. Nevertheless, backscatter communication networks based on ambient RF energy harvesting do not have scalability due to their dependance on other networks as energy sources. Thus they may not be suitable for implementing large-scale dense IoT. This motivates the design of WP-BC network architecture where WPT can deliver power much higher than that by energy harvesting and low-complexity backhaul-less PBs allow widespread deployment to power dense passive D2D links.

The work is based on the popular approach of designing and analyzing wireless networks using stochastic geometry (a survey can be found in e.g., [10]). Among various types of spatial point processes, *Poisson cluster process* (PCP), where *daughter* points form random clusters centered at points from a *parent Poisson point process* (PPP), are commonly used for modeling wireless networks with random cluster topologies arising from geographical factors or protocols for medium access control [11], [12]. In particular, in recent work on heterogeneous networks, PCPs have been frequently used to model the phenomenons of user clustering at hotspots [13] and the clustering of small-cell base stations (BSs) around macro-cell BSs [14]. In this work, the WP-BC network is also modeled as a PCP where PBs form the parent PPP and backscatter nodes are the clustered daughter points. This topology is motivated by the fact that only nodes sufficiently near PBs can harvest enough energy for operating circuits and powering transmission. Relying on WPT from PBs, nodes' transmission power depends on their distances from the nearest PBs. In contrast, in the conventional network models, transmis-

978-1-5090-1328-9/16/$31.00 ©2016 IEEE

sion power of BSs/nodes is independent of their locations. The location-dependent transmission power in the WP-BC network as well as other practical factors (e.g., circuit power and backscatter duty cycle) introduce new challenges for network performance analysis.

Recently, stochastic geometry has been also applied to model large-scale WPT networks building on existing network architectures including cellular networks [3], [15] and relay networks [16], [17]. In particular, the WP-BC network is similar to cellular networks with WPT considered in [3], [15] in that PBs are deployed to power passive nodes' transmissions. Nevertheless, the current work faces new theoretical challenges arising from a new network topology based on a PCP instead of PPPs in the prior work. Furthermore, practical factors arising from backscatter (e.g., duty cycle and reflection coefficient) also introduce a new dimension for network performance optimization.

To the best of our knowledge, the current work represents the first attempt to model and analyze a large-scale backscatter communication network using stochastic geometry. The theoretic contributions of this paper are summarized as follows. Based on the mentioned model, the performance of the WP-BC network are quantified in terms of 1) *success probability* for communication over a typical backscatter D2D link and 2) *transmission capacity* for measuring the spatial density of reliable active links. The analysis of the metrics are based on deriving the interference characteristic functionals and signal power distribution in the WP-BC network, which account for circuit power, duty cycle D, and reflection coefficient β of backscatter nodes. The success probability and network capacity are found to be concave functions of β and D, respectively, shedding light on the WP-BC network design by convex optimization.

II. Mathematical Models and Metrics

A. Network Model

The random WP-BC network is modeled using a PCP as follows. Let $\Pi = \{Y_0, Y_1, \cdots\}$ denote a PPP in the horizontal plane with density λ_p modeling the locations of PBs. Consider a cluster of mobile transmitting nodes centered at the origin, denoted as $\widetilde{\mathcal{N}} = \{X_0, X_1, \cdots, X_N\}$. The number of nodes, N, is a Poisson random variable (r.v.) with mean $\bar{c}$. The r.v., $X_n \in \mathbb{R}^2$, represents the location of the corresponding node and $\{X_n\}$ are independent and identically distributed (i.i.d.). For an arbitrary r.v. X_n, the direction is isotropic and the distance to the origin, $|X_n|$ [1], has one of two possible probability density functions (PDFs), resulting in the Matern and Thomas cluster process. Let the function $f : \mathbb{R}^+ \to \mathbb{R}^+$ denote the PDF of the distance from a cluster member's location to the cluster center, denoted as r, which is defined as follows:

$$\text{(Matern c.p.)} \quad f(r) = \begin{cases} \frac{1}{\pi a^2}, & 0 \le r \le a, \\ 0, & \text{otherwise}, \end{cases} \tag{1}$$

$$\text{(Thomas c.p.)} \quad f(r) = \frac{1}{2\pi\sigma^2} \exp\left(-\frac{r^2}{2\sigma^2}\right), \tag{2}$$

[1]Given $X \in \mathbb{R}^2$, $|X|$ denotes the Euclidean distance from X to the origin.

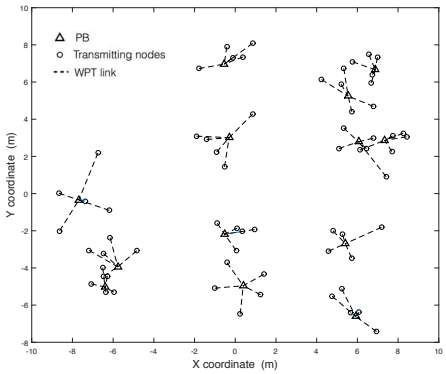

Figure 1: The spatial distribution of the WP-BC network modeled using the Thomas cluster process.

where a and σ^2 are positive constants representing the cluster radius and the variance, respectively. Let $\{\widetilde{\mathcal{N}}_Y\}$ denote a sequence of clusters constructed by generating an i.i.d. sequence of clusters having the same distribution as $\widetilde{\mathcal{N}}$ and translating them to be centered at the points $\{Y\} \in \Pi$. Then the process of transmitting nodes, denoted as $\tilde{\Phi}$, can be written as

$$\tilde{\Phi} = \bigcup_{Y \in \Pi} (\widetilde{\mathcal{N}}_Y + Y). \tag{3}$$

The density of $\tilde{\Phi}$ is $\lambda_p \bar{c}$. Fig.1 shows the network realization generated based on Thomas cluster process. Each transmitting node is paired with an intended receiving node that is located at a unit distance and in an isotropic direction. This generates a random spatial process modeling distributed D2D links.

Time is divided into slots of unit duration. Each slot is further divided into M mini-slots. In each slot, independent of others, a transmitting node randomly selects a single mini-slot to transmit signal by backscattering. This divides each slot into a backscatter phase and a waiting phase of durations $1/M$ and $(1 - 1/M)$, respectively (see more details in the following sub-section). The duty cycle, denoted as D, is given as $D = 1/M$. A transmitting node in a backscatter phase is called a *backscatter node*. Then the backscatter-node process, denoted as Φ, and a cluster of backscatter nodes centered at Y, denoted as $\mathcal{N}_Y$, can be obtained from $\tilde{\Phi}$ and $\widetilde{\mathcal{N}}_Y$ by independent thinning. As a result, Φ has the density of $\lambda_p \bar{c} D$ and the expected number of nodes in $\mathcal{N}_Y$ is $\bar{c}D$.

The channels are modeled as follows. PBs are equipped with antenna arrays and nodes have single isotropic antennas. Each PB beams a continuous wave (CW) to nodes in the corresponding cluster. Given beamforming and relatively short distances for efficient WPT, each WPT link can be suitably modeled as a channel with path loss but no fading [1]. The PB allocates transmission power of η for each node. As a result, with a typical PB at Y_0, the receive power at a typical node X_0 is given as $P_{X_0} = \eta g |X_0 - Y_0|^{-\alpha_1}$ where $g > 0$ denotes the beamforming gain and α_1 the path-loss exponent for WPT links. Due to beamforming, it is assumed that each node harvests negligible energy from other PBs and data signals compared with that from the serving PB. When transmitting, a node backscatters a fraction, called a *reflection coefficient* and denoted as $\beta \in [0, 1]$, of P_X such that the signal power received at the typical receiver at Z_0 is $\beta P_{X_0} h_{X_0}$ where

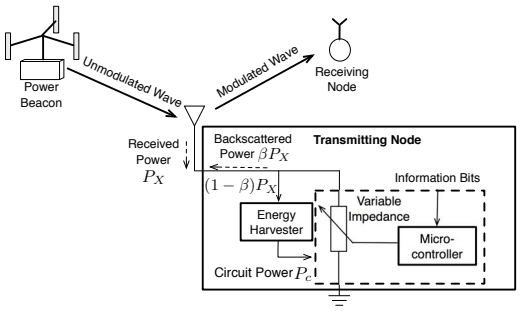

Figure 2: Wirelessly powered backscatter communication.

$h_{X_0} \sim \exp(1)$ models Rayleigh fading. A backscatter node may not be able to transmit if there is insufficient energy for operating its circuit as discussed in the sequel. Let Q_X denote the random on/off transmission power of the backscatter node X. The interference power measured at Z_0 can be written as

$$I = \sum_{X \in \Phi \setminus \{X_0\}} Q_X h_X |X - Z_0|^{-\alpha_2}, \tag{4}$$

where $\{h_X\}$ are i.i.d. $\exp(1)$ r.v.s modeling Rayleigh fading and α_2 represents the path-loss exponent for interference (D2D) links. It is worth to mention that the signal transmitted from PB is unmodulated carrier that appears as a DC level after down-conversion, which can be easily removed and thus not considered as interference as those modulated ones.

B. Backscatter Communication Model

The operation of WP-BC network is illustrated in Fig. 2. Consider the backscatter phase of an arbitrary slot. A transmitting node adapts the variable impedance (or equivalently its level of mismatch with the antenna impedance) shown in the figure so as to modulate the backscattered CW with information bits [5]. Given a backscatter node at X and the reflection coefficient β, the backscattered power is βP_X with the remainder $(1-\beta)P_X$ consumed by the circuit or harvested [18]. Next, for the waiting phase, the transmitting node withholds transmission and performs only energy harvesting. It is assumed that the circuit of each transmitting node consumes fixed power denoted as P_c in each time slot. To be able to transmit, a backscatter node has to harvest sufficient energy for powering the circuit, resulting in the following *circuit-power constraint*: $(1-\beta)P_X D + P_X(1-D) \geq P_c$. This gives

$$\text{(Circuit-power constraint)} \quad P_X \geq \frac{P_c}{1-\beta D}. \tag{5}$$

Consequently, a backscatter node transmits or is silent depending on if the constraint is satisfied.

C. Performance Metrics

The network performance is measured by two metrics. One is the probability of the event that the transmission over a typical D2D link is successful, called the *success probability* and denoted as P_s. Assuming an interference limited network, the condition for successful transmission is that the received signal-to-interference ratio (SIR) exceeds a fixed positive threshold θ. Under the circuit power constraint in (5), a transmission power of the typical transmitting node can be written as $Q_{X_0} = \beta \ell(P_{X_0})$ where the function $\ell(P)$ gives P if $P \geq P_c/(1-\beta D)$ or else is equal to 0. Similarly, the interference power in (4) can be rewritten as

$$I = \sum_{X \in \Phi \setminus \{X_0\}} \beta \ell(P_X) h_X |X - Z_0|^{-\alpha_2}. \tag{6}$$

Then the success probability is given as

$$P_s = \Pr\left(\beta \ell(P_{X_0}) h_{X_0} \geq \theta I\right). \tag{7}$$

The other metric is *transmission capacity* [10] denoted as C and defined as

$$C = \lambda_p \bar{c} D P_s. \tag{8}$$

The metric measures the density of reliable and active backscatter D2D links.

III. Interference and Signal Distributions

In this section, for the WP-BC network, the distributions of interference at the typical receiver and the signal transmission power for the typical backscatter node are analyzed. The results are used subsequently for characterizing network coverage and capacity.

A. Interference Characteristic Functionals

Let $\mathcal{C}(s)$ with $s > 0$ denote the characteristic functional of the interference power I given in (6): $\mathcal{C}(s) = \mathsf{E}\left[e^{-sI}\right]$. In this section, the characteristic functional is derived. Without loss of generality, consider a typical backscatter node at X_0 at the origin and the typical receiving node $Z_0 = z$. To facilitate derivation, I is decomposed into the power of *intra-cluster* and *inter-cluster* interference, denoted as I_a and I_b, respectively. Mathematically, $I = I_a + I_b$ where

$$I_a = \sum_{X \in \mathcal{N}_0 \setminus \{X_0\}} \beta \ell(P_X) h_X |X - z|^{-\alpha_2}, \tag{9}$$

$$I_b = \sum_{Y \in \Pi \setminus \{Y_0\}} \sum_{X \in \mathcal{N}_Y} \beta \ell(P_X) h_X |X - z|^{-\alpha_2}. \tag{10}$$

Note that in (10), the first summation is over all other PBs not affiliated with the typical backscatter node (corresponding to clusters of interferers) and the second summation is over the cluster of interferers centered at the PB Y.

The characteristic functionals of I_a and I_b are denoted as $\mathcal{C}_a(s)$ and $\mathcal{C}_b(s)$, respectively, which are defined similarly as $\mathcal{C}(s)$. They are derived as shown in the following two lemmas.

Lemma 1 (Intra-cluster interference)**.** Given $s \geq 0$, the characteristic functional of the intra-cluster interference power I_a is given as

$$\mathcal{C}_a(s) = \int_{\mathbb{R}^2} \exp\Big(-\bar{c} D q(s,y,z)\Big) f(|y|) dy,$$

where

$$q(s,y,z) = \int_{\mathbb{O}} \frac{1}{1 + (s\beta\eta g)^{-1} |x|^{\alpha_1} |x+y-z|^{\alpha_2}} f(|x|) dx, \tag{11}$$

and the set $\mathbb{O}$ arising from the *circuit power constraint* is defined as $\mathbb{O} = \left\{ x \in \mathbb{R}^2 \mid |x| \leq \left(\frac{\eta g (1-\beta D)}{P_c}\right)^{\frac{1}{\alpha_1}} \right\}$.

Proof: Please refer to the extended version [19]. □

Lemma 2 (Inter-cluster interference)**.** Given $s \geq 0$, the characteristic functional of the inter-cluster interference power I_b is given as

$$\mathcal{C}_b(s) = \exp\left(-\lambda_p \int_{\mathbb{R}^2} \left(1 - e^{-\bar{c}Dq(s,y,z)}\right) dy \right), \quad (12)$$

where $q(s, y, z)$ and the set $\mathbb{O}$ are defined in Lemma 1.

Proof: Please refer to the extended version [19]. □

B. Signal Distribution

Under the circuit-power constraint, there exists a threshold on the separation distance between a pair of PB and affiliated backscatter node:

$$d_0 = \left[\frac{\eta g(1-\beta D)}{P_c} \right]^{\frac{1}{\alpha_1}}, \quad (13)$$

such that the node's transmission power is zero if the distance exceeds the threshold. Then transmission power of the typical backscatter node, denoted as P_t, is given as $P_t = \beta\eta g|X_0 - Y_0|^{-\alpha_1}$ if $|X_0 - Y_0| \leq d_0$ or otherwise $P_t = 0$. The event of $P_t = 0$ corresponds that of (circuit) power outage. It follows that the *power-outage probability*, denoted as p_0, can be written as

$$p_0 = \Pr(P_t = 0) = 2\pi \int_{d_0}^{\infty} f(r) r dr. \quad (14)$$

For the case where the circuit-power constraint is satisfied,

$$\Pr(P_t \geq \tau) = 2\pi \int_0^{(\beta\eta g/\tau)^{\frac{1}{\alpha_1}}} f(r) r dr, \quad \tau \geq \frac{\beta P_c}{1-\beta D}. \quad (15)$$

Substituting the PDFs in (1) and (2) into (14) and (15) gives the following result.

Lemma 3 (Node transmission power)**.** The transmission power of a typical backscatter node has support of $\{0\} \cup [\frac{\beta P_c}{1-\beta D}, \infty]$. The power-outage probability, p_0, and the complementary cumulative distribution function (CCDF), denoted as $\bar{F}_t$, are given as follows.

– (**Matern cluster process**)

$$p_0 = \begin{cases} 1 - \left(\frac{d_0}{a}\right)^2, & d_0 < a, \\ 0, & \text{otherwise.} \end{cases}$$

$$\bar{F}_t(\tau) = \Pr(P_t \geq \tau) = \begin{cases} \frac{1}{a^2}\left(\frac{\beta\eta g}{\tau}\right)^{\frac{2}{\alpha_1}}, & \tau > \frac{\beta\eta g}{a^{\alpha_1}} \\ 1, & \text{otherwise,} \end{cases}$$

with $\tau \in [\frac{\beta P_c}{1-\beta D}, \infty]$.

– (**Thomas cluster process**)

$$p_0 = \exp\left(-\frac{d_0^2}{2\sigma^2}\right),$$

$$\bar{F}_t(\tau) = 1 - \exp\left(-\frac{1}{2\sigma^2}\left(\frac{\beta\eta g}{\tau}\right)^{\frac{2}{\alpha_1}}\right),$$

with $\tau \in [\frac{\beta P_c}{1-\beta D}, \infty]$.

A sanity check is as follows. The distance threshold d_0 in (13) is a monotone decreasing function of both βD and P_c. The reason is that increasing the duty cycle and reflection coefficient leads to less harvested energy thus adding the probability of circuit-power outage and improving the circuit power has the same effect. Consequently, the power-outage probability decreases with increasing d_0 for both cases in Lemma 3. Next, the CCDFs in Lemma 3 are observed to be independent of D but increase with growing β. The reason is that conditioned on the node transmitting, the transmission power depends only on the incident power from the PB scaled by β but is independent of the duty cycle.

IV. Network Coverage and Capacity

In this section, the coverage and capacity of the WP-BC network are characterized using the results derived in the preceding section.

A. Network Coverage

The network coverage is quantified by deriving the success probability, P_s defined in (7), as follows. The event of successful transmission by the typical backscatter node occurs under two conditions: 1) the circuit-power constraint in (5) is satisified and 2) under this condition, the receive SIR exceeds the threshold θ. Therefore, P_s can be written as

$$P_s = \Pr\left(P_t h_{X_0} \geq \theta I \mid P_t \neq 0\right) \Pr(P_t \neq 0). \quad (16)$$

Replacing the transmission power with its minimum value gives a lower bound on P_s as follows:

$$P_s \geq (1-p_0)\mathsf{E}\left[\exp\left(-\frac{\theta I(1-\beta D)}{\beta P_c}\right)\right].$$

Then the main result of the section follows by substituting the results derived in the preceding section.

Theorem 1 (Network coverage)**.** The *success probability* is bounded as

$$P_s \geq (1-p_0)\mathcal{C}\left(\frac{\theta(1-\beta D)}{\beta P_c}\right), \quad (17)$$

where $\mathcal{C}(s) = \mathcal{C}_a(s)\mathcal{C}_b(s)$ is the interference characteristic functional with $\mathcal{C}_a$ and $\mathcal{C}_b$ given in Lemma 1 and Lemma 2, respectively, and p_0 is the power outage probability specified in Lemma 3.

Remark 1 (Effects of p_0)**.** The success probability is observed to increase *linearly* with the *transmission probability* of a backscatter node, $(1-p_0)$, which agrees with intuition.

Remark 2 (Effects of β and D on network coverage)**.** The success probability P_s can be maximized over the reflection coefficient β. A too large or a too small value for β has a negative effect on network coverage (or the success probability). On one hand, increasing β not only adds the probability of circuit power-outage but also scales up transmission power for each node, which can lead to strong interference. On the other hand, β being too small leads to weak receive signal as well as larger effective interference set $\mathbb{O}$ given in (11). Both decrease

the success probability. Consider duty cycle D. A large duty cycle can result in larger circuit-power outage probability and dense interferers with strong interference, both reduce P_s.

B. Network Capacity

In this section, we consider a WP-BC network with close-to-full network coverage such that transmitted data is always successfully received almost surely. Using (16), the successful probability can be approximated as $P_s \approx 1 - p_0$. Accordingly, the transmission capacity defined in (8) reduces to the density of transmitting nodes:

$$C \approx \lambda_p \bar{c} D (1 - p_0). \tag{18}$$

Substituting the results in Lemma 3 gives Theorem 2.

Theorem 2 (Network capacity)**.** In the regime of close-to-full network coverage, the network transmission capacity can be approximated as follows.

– (**Matern cluster process**)

$$C \approx \frac{\lambda_p \bar{c} D}{a^2} \left[\frac{\eta g (1 - \beta D)}{P_c} \right]^{\frac{2}{\alpha_1}}.$$

– (**Thomas cluster process**)

$$C \approx \lambda_p \bar{c} D \left[1 - \exp\left(-\frac{1}{2\sigma^2} \left(\frac{\eta g (1 - \beta D)}{P_c} \right)^{\frac{2}{\alpha_1}} \right) \right].$$

First of all, the transmission capacity C is observed to be proportional to the density of backscatter nodes that is consistent with intuition.

Remark 3 (Effects of D and β on network capacity)**.** The parameters affect the transmission capacity in the mentioned regime by varying the transmitting-node density. In comparison, their effects on network coverage are not entirely the same and reflected in those on transmission probability and link reliability (see Remark 2). In the regime of almost-full network coverage, C decreases with the growing reflection coefficient β. The reason is that a large coefficient leads to less harvested energy and thereby reduces the transmitting-node density. In particular, C scales with β as $(1 - D\beta)^{\frac{2}{\alpha_1}}$. Next, increasing D has two opposite effects on the transmitting-node density, namely increasing the backscatter-node density but reducing transmission probability due to less harvested energy. Therefore, the capacity can be optimized over D. For instance, for the model based on the Matern cluster process, the maximum capacity is

$$\max_D C(D) = \frac{\lambda_p \bar{c} \alpha_1}{a^2 (2 + \alpha_1 \beta)} \left[\frac{2 \eta g}{P_c (2 + \alpha_1 \beta)} \right]^{\frac{2}{\alpha_1}}, \tag{19}$$

and the optimal duty cycle is given as $D^* = \min\left(1, \frac{\alpha_1}{2 + \alpha_1 \beta}\right)$. This assumes that D^* is within the constrained range discussed in the following remark. The capacity optimization for the case of Thomas cluster process is similar but more tedious.

Remark 4 (Constraints on D and β)**.** It is clear from Remark 2 that the consideration of the mentioned network operational regime constraints D and β to certain ranges to ensure link reliability. The capacity results in Theorem 2 holds only for the parameters falling in these ranges. The corresponding region for (β, D) can be derived by bounding the conditional probability in (16) by a positive value close to one. For instance, using Theorem 1, an inner bound of the region can be derived as

$$\left\{ (D, \beta) \in [0,1]^2 \mid \mathcal{C}\left(\frac{\theta (1 - \beta D)}{\beta P_c} \right) \geq 1 - \epsilon \right\}, \tag{20}$$

where the positive constant $\epsilon \approx 0$.

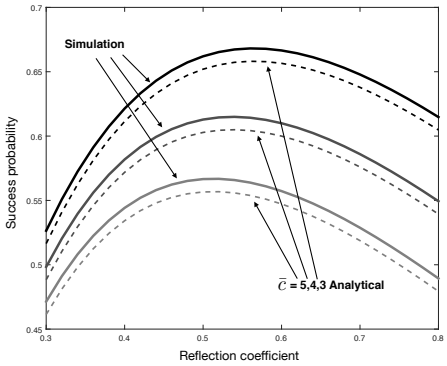

(a) Effect of the reflection coefficient

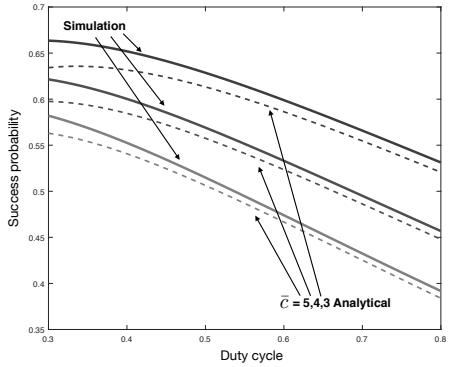

(b) Effect of the duty cycle

Figure 3: The effects of the backscatter parameters, namely the reflection coefficient and duty cycle, on the success probability for a variable expected number of backscatter nodes per cluster, $\bar{c} \in \{3, 4, 5\}$.

V. Simulation Results

The parameters for the simulation are set as follows unless stated otherwise. The PB transmission power η = 40 dBm (10 W) and circuit power is P_c = 7 dBm. The SIR threshold is set as $\theta = -5$ dB in the typical range for ensuring almost-full network coverage (see e.g., [20]). The path-loss exponents for WPT and communication links are α_1 = 3 and α_2 = 3, respectively. The backscatter reflection coefficient $\beta = 0.6$ and duty cycle $D = 0.4$. The PB density is $\lambda_p = 0.2$ /m^2 and the expected number of nodes in each cluster $\bar{c} = 3$. The transmission distances for D2D links are set as 1 m. The network model based on the Thomas cluster process is assumed with the parameter σ^2 = 4.

The curves of success probability versus the reflection coefficient and duty cycle are plotted in Fig. 3 for different values of $\bar{c}$. The curves based on the analytical results in

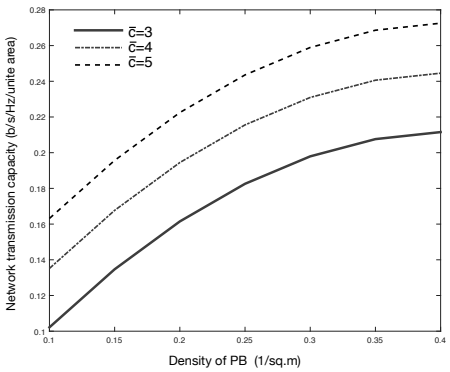

(a) Effect of the PB density

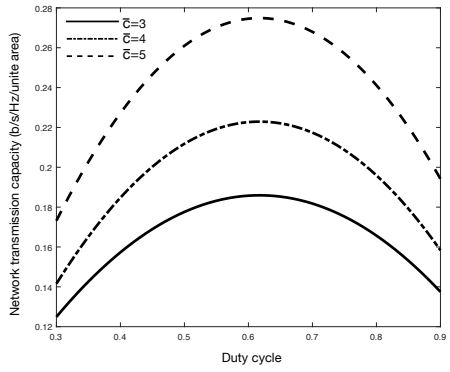

(b) Effect of the duty cycle

Figure 4: The effects of the PB density and duty cycle on the network capacity for a variable expected number of backscatter nodes per cluster, $\bar{c} \in \{3, 4, 5\}$

Theorem 1 are plotted for comparison. It is observed that the theoretical lower bounds are tight. For reflection coefficient β in Fig. 3(a), the curves show that the success probability is concave function of that parameter, which is consistent with the discussion in Remark 2. The optimal value for the reflection coefficient is observed to be about $0.5 - 0.6$. Consider duty cycle D in Fig. 3(b), the success probability decreases with improving D because of the higher density of interference and larger power-outage probability. Moreover, the lower bounds are relative not that tight when the values of D are small. The reason is smaller D leads to higher probability of transmission, so using $\frac{\beta P_c}{1-\beta D}$ to replace P_t gives a little larger gap.

The curves of network transmission capacity versus the PB density and the duty cycle are shown in Fig. 4 for different values of $\bar{c}$. In Fig. 4(a), when the density of PB is relatively small, the network capacity is observed to grow linearly with the PB density. For a large PB density, the capacity saturates as the network becomes dense and interference limited. Next, the network capacity is observed to be a concave function of the duty cycle. From Fig. 4(b), it can be observed that the capacity is a convex function of the duty cycle, which confirms Remark 3. The optimal duty cycle is almost identical (about 0.6) for different values of $\bar{c}$.

VI. Conclusion

In this work, we have proposed the new network architecture, namely the WP-BC network, for realizing dense backscatter communication networks using wireless power transfer enabled by PBs. A large-scale WP-BC network has been modeled using the PCP. Applying stochastic geometry theory, the success probability and the transmission capacity have been derived to quantify the performance of network coverage and capacity, respectively. In particular, the results relate the network performance to the backscatter parameters, namely the duty cycle and the reflection coefficient.

References

[1] K. Huang and X. Zhou, "Cutting the last wires for mobile communication by microwave power transfer," *IEEE Commun. Mag.*, vol. 53, pp. 86 – 93, Jun. 2015.

[2] S. Bi, C. Ho, and R. Zhang, "Wireless powered communication: opportunities and challenges," *IEEE Commun. Mag.*, vol. 53, pp. 117 – 125, Apr. 2014.

[3] K. Huang and V. Lau, "Enabling wireless power transfer in cellular networks: Architecture, modelling and deployment," *IEEE Trans. Wireless Commun.*, vol. 13, pp. 902–912, Feb. 2014.

[4] H. Stockman, "Communication by means of reflected power," *in Proc. IRE*, vol. 36, pp. 1196–1204, Oct. 1948.

[5] C. Boyer and S. Roy, "Backscatter communication and RFID: Coding, energy, and MIMO analysis," *IEEE Trans. Commun.*, vol. 62, pp. 770 – 785, Mar. 2014.

[6] G. Yang, C. Ho, and Y. Guan, "Multi-antenna wireless energy transfer for backscatter communication systems," *IEEE J. of Sel. Areas in Comm.*, vol. 33, pp. 2974–2987, Dec. 2015.

[7] J. Wang, H. Hassanieh, D. Katabi, and P. Indyk, "Efficient and reliable low-power backscatter networks," in *Proc. ACM SIGCOMM*, pp. 61–72, 2012.

[8] V. Liu, A. Parks, V. Talla, S. Gollakota, D. Wetherall, and J. Smith, "Ambient backscatter: wireless communication out of thin air," in *Proc. ACM SIGCOMM*, pp. 39–50, 2013.

[9] B. Kellogg, A. Parks, S. Gollakota, J. Smith, and D. Wetherall, "Wi-Fi backscatter: internet connectivity for RF-powered devices," in *Proc. of the ACM SIGCOMM*, pp. 607–618, 2014.

[10] M. Haenggi, J. Andrews, F. Baccelli, O. Dousse, and M. Franceschetti, "Stochastic geometry and random graphs for the analysis and design of wireless networks," *IEEE J. of Sel. Areas in Commun.*, vol. 27, pp. 1029–1046, Jul. 2009.

[11] R. Ganti and M. Haenggi, "Interference and outage in clustered wireless ad hoc networks," *IEEE Trans. Info. Theory*, vol. 9, pp. 4067–4086, Sep. 2009.

[12] K. Gulati, B. Evans, J. Andrews, and K. Tinsley, "Statistics of co-channel interference in a field of poisson and poisson-poisson clustered interferers," *IEEE Trans. Sig. Proc.*, vol. 58, pp. 6207–6222, Dec. 2010.

[13] Y. Chun, M. Hasna, and A. Ghrayeb, "Modeling heterogeneous cellular networks interference using poisson cluster processes," *IEEE J. of Sel. Areas in Commun.*, vol. 33, pp. 2182–2195, Oct. 2015.

[14] V. Suryaprakash, J. Moller, and G. Fettweis, "On the modeling and analysis of heterogeneous radio access networks using a poisson cluster process," *IEEE Trans. Wireless Commun.*, vol. 14, pp. 1035–1047, Feb. 2015.

[15] Y. Che, L. Duan, and R. Zhang, "Spatial throughput maximization of wireless powered communication networks," *IEEE J. of Sel. Areas in Commun.*, vol. 33, pp. 1534–1548, Aug. 2015.

[16] I. Krikidis, "Simultaneous information and energy transfer in large-scale networks with/without relaying," *IEEE Trans. Commun.*, vol. 62, pp. 900–912, Mar. 2014.

[17] P. Mekikis, A. Lalos, A. Antonopoulos, L. Alonso, and C. Verikoukis, "Wireless energy harvesting in two-way network coded cooperative communications: a stochastic approach for large scale networks," *IEEE Commun. Letters*, vol. 18, pp. 1011–1014, Jun. 2014.

[18] U. Karthaus and M. Fischer, "Fully integrated passive UHF RFID transponder IC with 16.7- mu;W minimum RF input power," *IEEE J. of Solid-State Circuits.*, vol. 38, pp. 1602–1608, Oct. 2003.

[19] K. Han and K. Huang, "Wirelessly powered backscatter communication networks: Modeling, coverage and capacity," *submitted to IEEE Trans. on Wireless Comm. (Avaiable: http://arxiv.org/abs/1605.05875)*.

[20] J. Andrews, F. Baccelli, and R. Ganti, "A tractable approach to coverage and rate in cellular networks," *IEEE Trans. Commun.*, vol. 59, pp. 3122–3134, Nov. 2011.